Molecular Vision 2024; 30:448-464 <http://www.molvis.org/molvis/v30/448>
Received 1 August 2024 | Accepted 28 December 2024 | Published 30 December 2024

Analysis of Smad3 in the modulation of stromal extracellular matrix proteins in corneal scarring after alkali injury

Suneel Gupta,[1,2] Eric Zhang,[1,3] Sampann Sinha,[1,2] Lynn M. Martin,[1,2] Thomas S. Varghese,[1,3] Nathan G. Forck,[1,2] Prashant R. Sinha,[1,2] Aaron C. Ericsson,[4] Nathan P. Hesemann,[1,3] Rajiv R. Mohan[1,2,3]

[1]Harry S. Truman Memorial Veterans' Hospital, Columbia, MO; [2]Departments of Veterinary Medicine & Surgery and Biomedical Sciences, College of Veterinary Medicine, University of Missouri, Columbia, MO; [3]Mason Eye Institute, School of Medicine, University of Missouri, Columbia, MO; [4]Departments of Veterinary Pathobiology, College of Veterinary Medicine, University of Missouri, Columbia, MO

Purpose: During ocular trauma, excessive proliferation and transdifferentiation of corneal stromal fibroblasts cause haze/fibrosis in the cornea. Transforming growth factor β (TGFβ) plays a key role in corneal fibrosis through the Smad signaling pathway. The aberrant activity of TGFβ signaling during ocular trauma (viz. mechanical, infectious, chemical, or surgically altered TGFβ/Smad signaling) leads to regulating the predominant expression of myogenic proteins and the extracellular matrix (ECM). We sought to investigate the functional role of Smad3 in corneal wound repair and stromal ECM assembly using $Smad3^{+/+}$ wild-type and $Smad3^{-/-}$ deficient mice.

Methods: Corneal injury was introduced with the topical application of an alkali-soaked 2-mm filter disc on the central cornea in the $Smad3^{+/+}$ (C57BL/6J) and $Smad3^{-/-}$ (129-$Smad3^{tm1Par}$/J) mouse strains. Slit-lamp and stereo microscopy were used for clinical assessment and corneal haze grading in live animals. Hematoxylin and eosin and Masson's trichrome staining were used to study comparative morphology and collagen level alterations between the groups. Real-time qRT-PCR, western blot, and immunohistochemistry were used to measure changes in profibrotic genes at the mRNA and protein levels.

Results: Slit-lamp clinical exams and stereo microscopy detected notably less opaque cornea in the eyes of $Smad3^{-/-}$ compared with $Smad3^{+/+}$ mice at 3 weeks ($p<0.01$) in live animals. Corneal tissue sections of $Smad3^{-/-}$ mice showed significantly fewer α-smooth muscle actin-positive cells compared with those of the $Smad3^{+/+}$ animals ($p<0.05$). The corneas of the $Smad3^{-/-}$ mice showed significantly lower mRNA levels of pro-fibrotic genes, α-smooth muscle actin, fibronectin, and collagen I ($p<0.05$, $p<0.01$, and $p<0.001$). In addition, the matrix metalloproteinase and tissue inhibitors of metalloproteinase levels were significantly increased ($p<0.001$) in the corneal tissue during alkali injury in both $Smad3^{+/+}$ wild-type and $Smad3^{-/-}$ deficient mice.

Conclusions: The significant changes in profibrotic genes and stromal ECM proteins revealed a direct role of Smad3 in stromal ECM proteins and TGFβ/Smad-driven wound healing. Smad3 appears to be an attractive molecular target for limiting abnormal stroma wound healing to treat corneal fibrosis in vivo.

The cornea is the clear, dome-shaped outermost layer of the eye. The avascular and transparent nature of the corneal tissue makes it a good model for understanding wound healing events [1-5]. Ocular trauma resulting from various corneal insults (such as mechanical, surgical, and chemical injuries) is a serious clinical problem worldwide [6-8]. Any of these traumatic impairments to the ocular tissue can compromise the normal transparency and curvature of the cornea [3-8]. Transdifferentiation of corneal stromal fibroblasts to myofibroblasts is an important event during trauma and plays a key role in extracellular matrix (ECM) protein secretion [9-11]. Exert contraction across the ECM results in tissue architecture alteration and impaired function, leading to corneal fibrosis pathology and corneal scarring [9-14]. Corneal scarring after trauma/infection impairs vision in 4% of Americans and accounts for 7% of the world's blindness. Over 23 million people globally, including many children, have corneal fibrosis in one eye and 4.9 million in both eyes [15-19]. Ocular trauma and corneal ulceration cause approximately 1.5–2.0 million new cases of monocular corneal blindness each year. In addition, approximately 1.4 million children have blindness worldwide, associated with lower socioeconomic class and suffering from socioeconomic deprivation [16-20]. The transdifferentiation of fibroblasts into contractile and secretory myofibroblasts and their persistence in the corneal tissue are the common sequelae of corneal fibrosis [11-14]. The transdifferentiation of corneal stromal fibroblasts into myofibroblasts and deposition of ECM proteins in the stroma lead to the formation of a collagen-based scar [12-14,21-23].

Correspondence to: Rajiv R. Mohan, Department of Ophthalmology and Molecular Medicine, University of Missouri, 1600 E. Rollins St., Columbia, MO 65211; email: mohanr@health.missouri.edu

During wound healing, transforming growth factor β (TGFβ) signals, through canonical and/or noncanonical signaling pathways [24-28], are known to promote conversion of corneal stromal fibroblasts to myofibroblasts, enhance ECM protein synthesis, and promote translocation of suppressors mothers against decapentaplegic (Smads) [29-32]. In addition, they can alter the activity of proteases, including matrix metalloproteinases (MMPs) and tissue inhibitors of metalloproteinases (TIMPs) [33-39]. MMPs, proteolytic enzymes, are essential in wound healing and have roles in fibrosis, ECM remodeling, and active wound healing [33-39]. The activities of MMPs are tightly regulated by gene expression, activation of zymogens (cysteine switch mechanism), and inactivation of enzymes with inhibitors such as endogenous TIMPs [33-39]. A proper balance of MMP and TIMP activities is critical for ECM homeostasis [35-39]. Smad proteins are unique transducers of the TGFβ family receptor serine-threonine kinases and phosphorylation of regulatory Smads (R-Smads; Smad2 and Smad3), with common mediator Smad (co-Smad; Smad4) and translocation of the Smad complex to the nucleus playing a predominant role in the activation of TGFβ-dependent signaling and their target molecules during fibrosis [25-31]. R-Smad expression and activity/function are tightly and precisely controlled by post-translational modifications, including (de)phosphorylation, (de)ubiquitylation, sumoylation, deacetylation, methylation, and ADP-ribosylation [32]. Our group demonstrated that targeted Smad7 (inhibitory Smad) gene transfer in stroma via adeno-associated vectors reduced corneal fibrosis in an alkali-injured rabbit cornea in vivo [7]. Based on the Smad7 overexpression gene therapy findings, we hypothesized that Smads are the key regulators in corneal wound healing and directly influence the TGFβ-dependent pathway to regulate the stromal ECM proteins during wound healing events. In the present study, we used Smad3$^{+/+}$ wild-type (C57BL/6J) and Smad3$^{-/-}$ deficient mice (129-Smad3^{tm1Par}/J) to establish the direct role of Smad3 in corneal wound healing and stromal ECM proteins. The objective of this study was to uncover the direct role of Smad3 in corneal wound healing and stromal ECM protein regulation using the loss-of-function approach with a Smad3$^{-/-}$ deficient mouse model.

METHODS

Reagents, chemicals, and surgical supplies: Standard research-grade chemicals and reagents were used to perform this study. Sodium hydroxide (NaOH), paraformaldehyde solution, Triton X100, and bovine serum albumin were purchased from Sigma–Aldrich, St. Louis, MO. Two-methyl butane and antifade mounting 4′,6-diamidino-2-phenylindole dihydrochloride medium (cat # H1200, Vector Laboratories) were obtained from Thermo Fisher, Grand Island, NY. Topical artificial tears were obtained from Rugby Laboratories, Livonia, MI. Hematoxylin and eosin (H&E) solutions were procured from StatLab Medical Products, McKinney, TX. Sterile Weck-Cel ophthalmic spears were purchased from Beaver-Visitec International Inc., Waltham, MA. Surgical forceps and sharp Westcott scissors were purchased from World Precision Instruments Inc., Sarasota, FL. Ketamine hydrochloride (JHP Pharmaceuticals, LLC, Rochester, MI), xylazine hydrochloride (XylaMed, Bimeda Inc., Le Sueur, MN), topical 0.5% proparacaine hydrochloride (Alcon, Ft. Worth, TX), and pentobarbital (Diamondback Drugs, Scottsdale, AZ) were obtained from Harry S. Truman VA Medical Center, Columbia, MO.

Ethics statement: All mice experimental procedures were approved by the Institutional Animal Care and Use committees of the University of Missouri (MU) and the Harry S. Truman Memorial Veterans' Hospital. The study was conducted in accordance with the ARVO recommendations for animal experimentation, and data were presented in accordance with the ARRIVE guidelines.

Animals: In this study, Smad3$^{+/+}$ (C57BL/6J) and Smad3$^{-/-}$ (129-Smad3^{tm1Par}/J) deficient mice 8–12 weeks in age in groups of both male and female sex were used, despite our previous work showing that sex does not play an important role during corneal wound healing [40]. Smad3$^{-/-}$ (129-Smad3^{tm1Par}/J) mice were generated from a breeding pair procured from Dr. Aaron C. Ericsson, Department of Veterinary Pathobiology, MU (Columbia, MO) [41]. Wild-type C57BL/6J (Smad3$^{+/+}$) mice were purchased from the Jackson Laboratory, Bar Harbor, ME. Both, Smad3$^{+/+}$ and Smad3$^{-/-}$ mice were used to elucidate the essential and functional role of Smad3 in corneal wound healing and stromal remodeling in vivo. Smad3-deficient mice (Smad3$^{-/-}$; n=12) and wild-type C57BL/6J mice (Smad3$^{+/+}$; n=12) (genetic background C57BL/J6) were bred by homozygote breeding. Smad3$^{-/-}$ deficiency was confirmed by a polymerase chain reaction using specific primers for Smad3$^{-/-}$ mice (as listed in Table 1) and horizontal 2.0% agarose gel [41].

Scar induction in Smad3$^{+/+}$ and Smad3$^{-/-}$: Mice were anesthetized with an intraperitoneal injection of a ketamine hydrochloride (100 mg/kg) and xylazine hydrochloride (10 mg/kg) cocktail. A single drop of topical anesthetic, proparacaine hydrochloride (0.5%), was instilled into the eye before alkali wounding to reduce pain and discomfort to the animal before the scar induction, clinical assessment, and clinical biomicroscopy. Corneal manipulations and scar induction procedures were performed under a surgical dissecting microscope as

reported previously [42-44]. Mice were thermally supported throughout the procedure and during the anesthetic recovery period. For scar induction, 20 µl of NaOH solution (0.5 M) was applied with a 2-mm-diameter filter paper disc (P8, Filter Paper, Fisher Brand, Fisher Scientific, Pittsburgh, PA) and placed onto the central cornea. The alkali-soaked filter disc contact with the corneal epithelium was maintained for 30 s as reported previously [42-44]. Thereafter, the eyes were copiously washed with a balanced salt solution to remove all NaOH traces. All in vivo experimental manipulations and imaging procedures were performed by keeping the experimental conditions constant to avoid variation and increase reproducibility. Both eyes were kept lubricated with artificial tears during the entire procedure to prevent corneal desiccation.

Slit-lamp corneal imaging for fibrosis assessment: After alkali scar induction, all mice underwent clinical eye examinations and corneal imaging at regular intervals (up to 3 weeks) for the assessment of scaring and for biomicroscopy images under general anesthesia. A wide-beam slit-lamp microscope (Leica DM 4000B, Leica Microsystems Inc., Buffalo Grove, IL) equipped with a digital camera (SpotCam RT KE, Diagnostic Instruments Inc., Sterling Heights, MI) was used to record wound progression in mouse corneal tissue [42-44]. At the time of haze evaluation, more than five images per animal at each time point were taken from both eyes to capture the fine corneal details. The scarring was graded according to Fantes haze score in an independent blinded manner as reported previously [6,7,45,46]. Briefly, naïve or completely clear corneas were graded 0; during the slit-lamp biomicroscopic evaluations, the presence of fine traces of haze during the tangential illumination of corneal tissue was graded 0.5; more prominent haze but not interfering with the visibility of fine iris details was graded 1; sufficient haze causing mild obscuration of iris detail was graded 2; sufficient haze causing moderate obscuration of the iris and lens was graded 3; and prominent haze with complete opacification of the corneal tissues was graded 4 in the traumatized injury zone.

The corneal epithelium defect/erosion was assessed using the fluorescein eye test under a cobalt blue light and recorded under a green fluorescent protein filter-equipped fluorescence microscope (Leica DM 4000B, Leica Microsystems Inc.) equipped with a digital camera (SpotCam RT KE, Diagnostic Instruments Inc.) as reported previously [47-49]. In this test, fluorescein uptake occurs in damaged corneal epithelium, and normal epithelium shows no dye under the green fluorescent protein filter/cobalt blue light.

Intraocular pressure (IOP) assessment: To determine the impact of Smad3 gene deficiency on aqueous humor regulation, intraocular pressure (IOP) measurement was evaluated using a handheld tonometer (iCare TONOLAB tonometer; TV02). All IOP measurements were performed between 9 AM and 11 AM to minimize normal diurnal variations and recorded by one operator to avoid operator-based variations [46-49].

Corneal tissue collection: Mice were humanely euthanized with an intraperitoneal injection of pentobarbital (150 mg/kg) while under general anesthesia at the termination point. Eyes were enucleated with surgical forceps and Westcott scissors under a dissecting microscope. Corneas were used for immunofluorescence, mRNA, and protein studies. Eyes were immediately placed into molds containing optimal cutting temperature compound and snap-frozen in a container of 2-methyl butane immersed in liquid nitrogen as reported previously [42-44]. Frozen tissues were maintained at −80 °C until sectioning and further evaluation. Tissues were sectioned at 8-µm thickness with a cryo-microtome, mounted on glass microscopic slides, and preserved at −80 °C for subsequent analysis.

Hematoxylin and eosin (H&E) histological studies: The mouse corneal tissue sections of both naïve and alkali-injury $Smad3^{+/+}$ and $Smad3^{-/-}$ were subjected to H&E staining to examine the gross morphology, cellular infiltration, and ECM alterations. H&E staining was performed in our laboratory using the protocol reported previously [42-44,47-51]. Additionally, corneal sections were sent to the MU Veterinary Medical Diagnostic Laboratory for H&E histology.

Masson's trichrome staining for collagen-level assessment: The mouse corneal tissue sections of both naïve and alkali-injury $Smad3^{+/+}$ and $Smad3^{-/-}$ were subjected to Masson's

Table 1. List of primers used for SMAD3+/+ and SMAD3−/− genotyping.

Primer		Sequence (5′-3′)	Nucleotides
Smad3 ex 2	Forward	GCACAGCCACCATGAATTAC	20
	Reverse	CCCAAGAGAGACACAACAGAG	21
Lac z	Forward	TTCACTGGCCGTCGTTTTACAACGTCGTGA	30
	Reverse	ATGTGAGCGAGTAACAACCCGTCGGATTCT	30

trichrome staining to evaluate alterations in collagen, a primary component of the ECM. Masson's trichrome staining was performed independently within the laboratory and by the MU Veterinary Medical Diagnostic Laboratory using a previously reported protocol [42-44,47-51].

Corneal immunofluorescence imaging: The corneal sections were used for localization and characterization of proteins under a fluorescence microscope as reported previously [42-44]. Briefly, the corneal tissue sections were washed three times with 1× phosphate-buffered saline for 5 min and incubated and blocked with 5.0% bovine serum albumin for 1 h. Tissue sections were then placed in a 1:100 dilution of a specific primary antibody (α-smooth muscle actin [α-SMA]: Cat# PA5–32587; Smad3: Cat# SC101154; and CD11b: Cat#550282) overnight at 4 °C and then washed with 1× phosphate-buffered saline for 5 min three times. Tissue sections were further incubated in secondary antibody Alexa Fluor™ 488 (Cat# A21206), Alexa Fluor™ 594 (Cat# A21135), or Alexa Fluor™ 594 (Cat# A21209) at 1:1000 dilution and mounted with 4′,6-diamidino-2-phenylindole dihydrochloride antifade medium. The stained corneal tissue sections were viewed and photographed with a fluorescence microscope equipped with a digital camera as reported previously [42-44,47-51].

Protein expression western blot analyses: The corneal protein lysates were subjected to characterization of specific proteins. Protein lysates were prepared by homogenizing corneas in Pierce RIPA buffer containing a protease inhibitor cocktail (Thermo Fischer Scientific) and quantified by the Bradford assay as described previously [42-51]. Samples were resolved on 4%–12% sodium dodecyl sulfate (SDS) polyacrylamide gel, transferred on a polyvinylidene fluoride membrane, incubated with primary antibodies (α-SMA: Cat # M0851; TIMP-1: Cat # AF980-SP; TIMP-2: Cat # D18B7; MMP-2: Cat # SC13594; MMP-9: Cat # SC13520; and GADPDH: Cat # 47,724) followed by corresponding horseradish peroxidase-conjugated secondary antibodies (HRP-conjugate; Cat # SC2005; Cat # 31,460), and developed with SuperSignal ELISA Femto maximum sensitivity substrate (Cat # 37,075) reagents. The blots were imaged and quantified using the iBright CL1500 imaging system, iBright analysis software (Invitrogen, Thermo Fischer Scientific), and NIH ImageJ (ImageJ 1.50i).

MMP detection using zymography: The expression of pro- and active isoforms of matrix metalloproteinases (MMP) protein was detected using gelatin zymography in the presence of 0.1% gelatin under nonreducing conditions as reported previously [25]. Briefly, a 20-µL sample was prepared by mixing total protein lysates (30 µg), Tris-glycine SDS sample buffer (10 µL), and deionized water. Samples were loaded on the 10% SDS polyacrylamide gel (Life Technologies, Novex, Carlsbad, CA) in the presence of 0.1% gelatin and were used under nonreducing conditions at a constant voltage (150 V; for 120 min) in a cold room. The gel was washed and developed using the zymography reagents. The developed gel was stained with SimplyBlue SafeStain diluted as per the vendor's instructions. Digital quantification of zymograms was performed using NIH ImageJ software (ImageJ 1.50i).

Statistical analysis: Statistical analysis was performed using GraphPad Prism 9.2 software (GraphPad Software, La Jolla, CA). A Student *t* test, Wilcoxon rank sum test, or Mann–Whitney tests were used to determine the statistical significance during data analysis of different experiments for biologic validation. The data are presented as the average mean ± standard error (SEM). In statistical analysis, $p \leq 0.05$ was considered significant.

RESULTS

Smad3-deficient strain validation: $Smad3^{-/-}$ deficiency in mice was confirmed by a standard polymerase chain reaction using specific primers for $Smad3^{-/-}$ mice as listed in Table 1. The agarose gel (2.0%) showed a band at 364 bp, confirming the $Smad3^{-/-}$ strain (Smad deficient; Figure 1A), whereas the $Smad3^{+/+}$ strain (wild type; Figure 1B) showed a band at 227 bp.

Smad3 gene deficiency regulates corneal scarring: Age-matched $Smad3^{+/+}$ (C57BL/6J, wild type) and $Smad3^{-/-}$ (Smad3) deficient mice (both male and female) were used to study the functional role of Smad3 during alkali-induced trauma for corneal scarring in vivo. The corneal scarring was assessed throughout the study period using slit-lamp microscopy observations in live animals and graded on Fantes scale (Figure 2). The subjective clinical slit-lamp and stereo microscopy evaluations exhibited intensified prominent scarring in the corneal tissues of $Smad3^{+/+}$ mice (Figure 2C,D) compared with $Smad3^{-/-}$ mice (Figure 2G,H) at day 7 and day 21, respectively. The $Smad3^{+/+}$ mouse corneas showed significantly increased scarring (1.6±0.48 fold; $p<0.001$) compared with the $Smad3^{-/-}$ mouse corneas on the Fantes haze scale (Figure 2I). The decreased corneal scarring in $Smad3^{-/-}$ deficient mouse corneas indicates the direct role of Smad3 in corneal scarring. The age-matched $Smad3^{+/+}$ (C57BL/6J mouse strain) and $Smad3^{-/-}$ (129-$Smad3^{tm1Par}$/J mouse strain) corneal tissue of both male and female mice during our clinical evaluation did not show any signs of opacity or other ocular alterations before alkali injury (naïve controls of both strains), as shown by representative slit-lamp microscopic images (Figure 2A,E). Tonometry analyses of

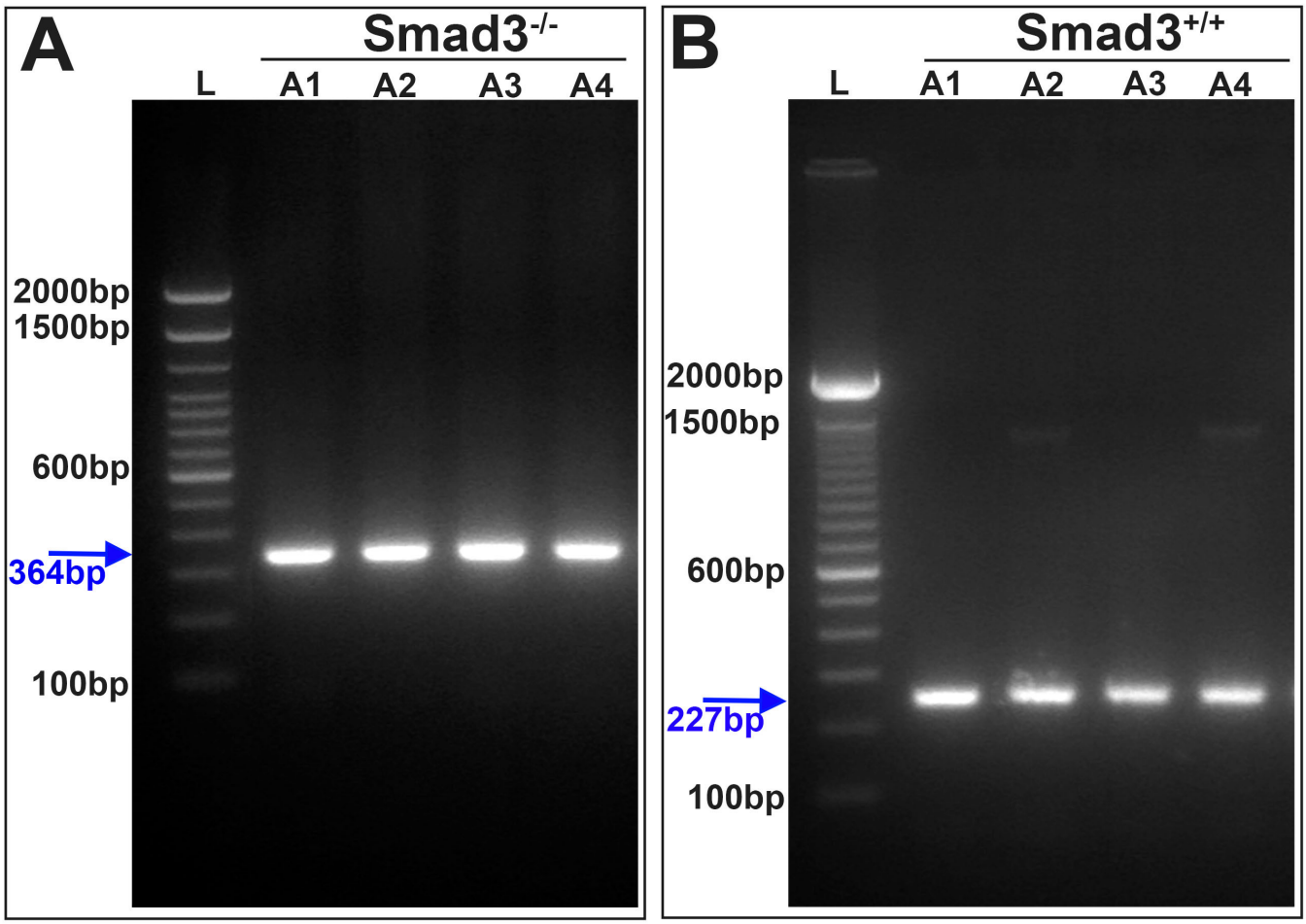

Figure 1. The 2% agarose gel validates the genotype of Smad3$^{-/-}$ and Smad3$^{+/+}$ mouse strains. **A:** The band at 364 bp confirms the Smad3$^{-/-}$ mouse strain in the representative gel image in A1-A4 different mice of Smad3$^{-/-}$ strain genomic DNA samples. **B:** The band at 227 bp confirms the Smad3$^{+/+}$ mouse strain in the representative gel image in A1-A3 different mice of Smad3$^{+/+}$ strain genomic DNA samples. L = 100 bp DNA ladder, bp = base pair.

mice did not show any statistically significant differences in the IOP of both strains in naïve and post-alkali injury conditions (Table 2). As expected, significant alteration in the corneal IOP was observed on day 1 after alkali injury due to initial alkali trauma to the corneal tissue. No significant changes were recorded in IOP at later time points from day 3 to day 21. The corneal re-epithelization was not impacted in Smad3$^{+/+}$ and Smad3$^{-/-}$ mouse corneal tissue, as indicated by fluorescein eye imaging in naïve and injured mouse corneas in a time-dependent epithelial assessment (Figure 3).

Smad3 gene deficiency tailored the inflammatory protein expression: The effect of Smad3 gene deficiency was evaluated by using the inflammatory marker CD11b protein expression (Figure 4). The post-injury group of animal corneal tissue sections of strains Smad3$^{+/+}$ and Smad3$^{-/-}$ showed notably enhanced CD11b protein expression (Figure 4C,D) compared with the naïve group of animal corneal tissue sections of strains Smad3$^{+/+}$ and Smad3$^{-/-}$ (Figure 4A,B) at day 21. However, Smad3 deficiency does not seem to have any significant impact on inflammatory response.

Smad3 critically regulates profibrotic TGFβ responses in wound healing: To test the postulate that Smad3 deficiency decreases the expression of pro-fibrotic markers in the cornea during active wound healing, the mRNA levels of fibronectin (FN), collagen 1, collagen 3, and collagen 4 were quantified in Smad3$^{-/-}$ mouse corneal tissue and compared with those of Smad3$^{+/+}$ mouse corneal tissue (Figure 5). The results of the mRNA expression study revealed a significant reduction in FN (Figure 5A; $p<0.001$), collagen 1 (Figure 5B; $p<0.01$), collagen 3 (Figure 5C; $p<0.05$), and collagen 4 (Figure 5D; $p<0.01$) and evidenced the direct role of Smad3 in TGFβ1-mediated stromal modulation during fibrosis. The mRNA

Table 2. IOP of naïve and post-alkali injury Smad3$^{+/+}$ and Smad$^{-/-}$ mice.

Intraocular pressure (IOP; mm Hg)				
	Naïve		Injured	
Days	Smad3$^{+/+}$	Smad3$^{-/-}$	Smad3$^{+/+}$	Smad3$^{-/-}$
Day 0	15.3±1.2	15.7±0.7	16.3±1.4	15.3±0.7
Day 1	14.7±0.3	14.0±1.1	20.3±0.9	18.8±1.2
Day 3	15.7±1.2	16.0±2.0	16.3±0.9	15.8±0.9
Day 7	15.3±1.3	15.3±1.3	15.7±1.9	14.0±0.6
Day 14	16.7±0.7	15.0±.1.0	15.8±1.2	15.0±0.6
Day 21	14.7±0.9	16.0±.0.6	16.0±1.7	16.3±1.2

Data were expressed in mean ± SEM; IOP=intraocular pressure.

expression profile of pro-fibrotic gene expression reveals that Smad3 gene deficiency directly regulates the downstream targets of TGFβ/Smad signaling.

To further support our lead hypothesis—a direct role of Smad3 in cellular differentiation during corneal wound healing—the corneal fibrosis marker α-SMA was used to show the protein expression between the Smad3$^{+/+}$ and Smad3$^{-/-}$ mice in naïve and injured corneas (Figure 6). The mRNA expression of α-SMA was significantly increased ($p<0.0001$) in the Smad3$^{+/+}$ mouse injured corneas compared with Smad3$^{-/-}$ mouse injured corneas (Figure 6A). The protein expression of α-SMA was also increased significantly, as shown by immunofluorescence staining (Figure 6B) and western blot analysis (Figure 6C,D), in Smad3$^{+/+}$ mouse injured corneas compared with Smad3$^{-/-}$ mouse injured corneas collected after euthanasia after alkali trauma on day 21. The western blot analysis data were corroborated with the mRNA and immunofluorescence staining and indicated that Smad3$^{-/-}$ group corneal tissue lysates showed a 2.16±0.56-fold reduction in α-SMA expression compared with Smad3$^{+/+}$ mouse group corneal tissue (Figure 6D).

Smad3 linkage in corneal stromal remodeling and ECM regulation during active wound healing: To study the morphological and structural changes in corneal tissues, Smad3$^{-/-}$ and Smad3$^{+/+}$ naïve and post-alkali injured mouse corneal tissue sections were subjected to H&E (Figure 7A) and Masson's trichrome staining (Figure 7B). No morphological alterations were observed in Smad3$^{-/-}$ and Smad3$^{+/+}$ naïve mouse corneal tissue sections (Figure 7A a,b). However, Smad3$^{-/-}$ mouse post-alkali injury corneal tissue sections showed less stromal cellular infiltration and distorted collagen lamellae compared with Smad3$^{+/+}$ mouse day 21 post-alkali injury corneal tissue sections (Figure 7A c,d).

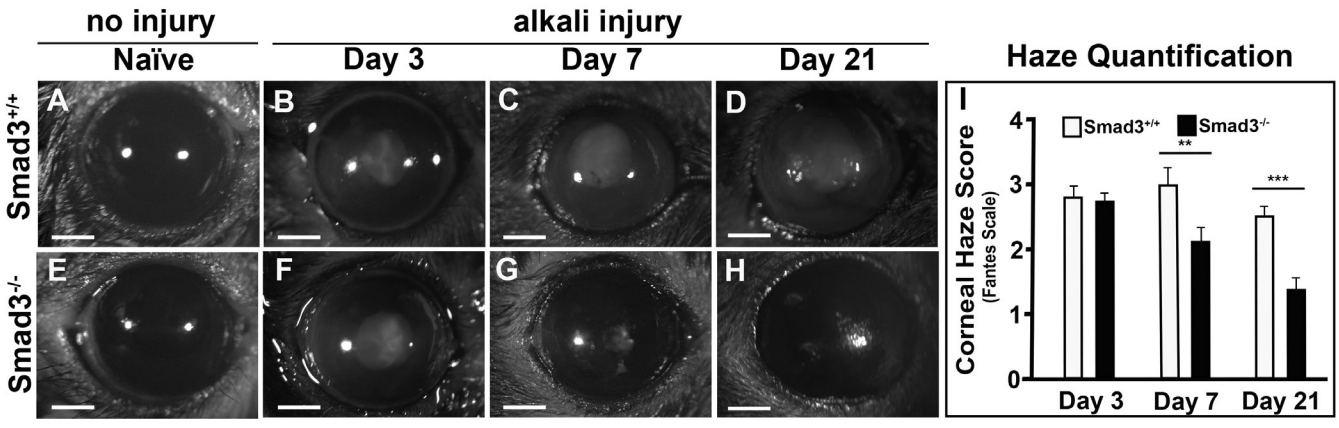

Figure 2. Smad3 gene deficiency reduced corneal haze in mice after alkali injury. The representative stereomicroscopic mouse corneal tissue images show the **A:** naïve; **B:** day 3; **C:** day 7; and **D:** day 21 post-alkali haze formation in Smad3$^{+/+}$ mouse strain corneal tissue. The stereomicroscopic mouse corneal tissue images show the **E:** naïve; **F:** day 3; **G:** day 7; and **H:** day 21 post-alkali haze formation in Smad3$^{-/-}$ mouse strain corneal tissue. **I:** The haze quantification graph shows that corneal haze was significantly reduced in Smad3$^{-/-}$ compared with Smad3$^{+/+}$ mouse corneal tissue (**p<0.01, ***p<0.001, scale bar = 0.5 mm).

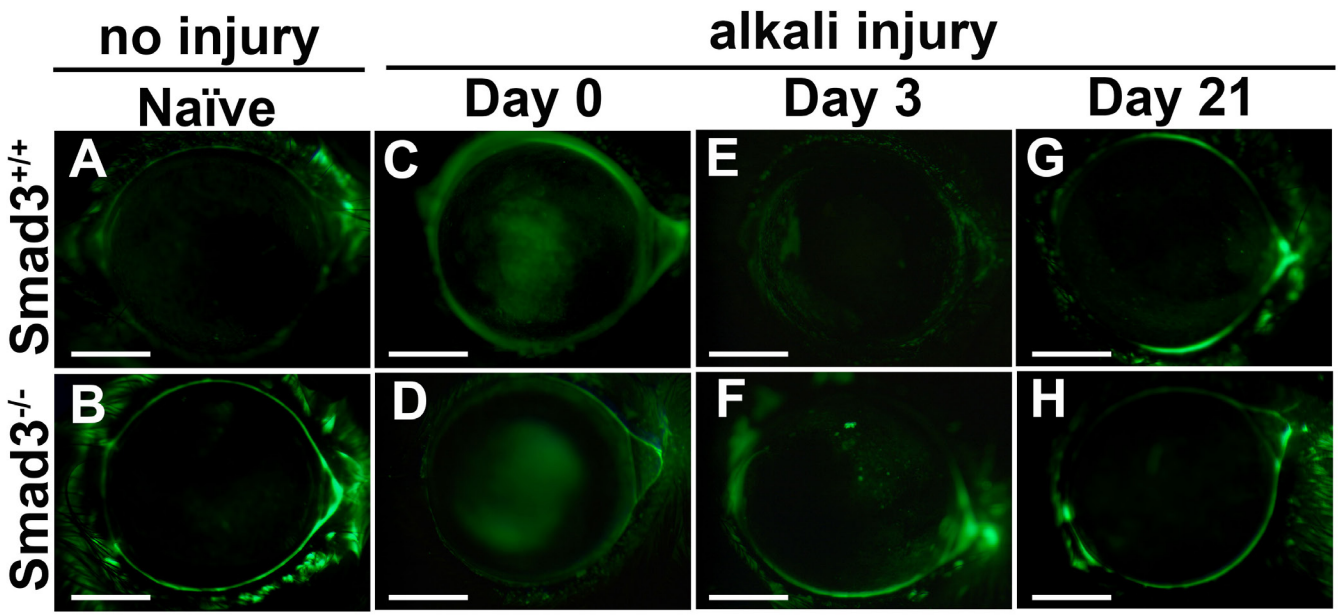

Figure 3. Smad3 gene deficiency does not alter the corneal epithelium. **A:** Smad3$^{+/+}$ naïve mouse corneal tissue; **B:** Smad3$^{-/-}$ naïve mouse corneal tissue; **C:** Smad3$^{+/+}$ alkali-injured mouse corneal tissue at day 0; **D:** Smad3$^{-/-}$ alkali-injured mouse corneal tissue at day 0; **E:** Smad3$^{+/+}$ alkali-injured mouse corneal tissue at day 3; **F:** Smad3$^{-/-}$ alkali-injured mouse corneal tissue at day 3; **G:** Smad3$^{+/+}$ alkali-injured mouse corneal tissue at day 21; and **H:** Smad3$^{-/-}$ alkali-injured mouse corneal tissue at day 21. The gross examination shows no alteration in the corneal epithelium of both strains of Smad3$^{+/+}$ and Smad3$^{-/-}$ naïve and alkali-injured corneas in a time-dependent manner. Scale bar = 0.5 mm.

The Masson's trichrome staining data were corroborated with H&E staining. No noticeable changes were perceived in the collagen level of Smad3$^{-/-}$ and Smad3$^{+/+}$ naïve mouse corneal tissue sections (Figure 7B a,b). Additionally, Smad3$^{-/-}$ mouse post-alkali injury corneal tissue sections showed less intensity of blue color, indicating better stromal reorganization and collagen lamellae compared with Smad3$^{+/+}$ mouse day 21 post-alkali injury corneal tissue sections (Figure 7B c,d).

Effects of Smad3 gene deficiency on TGFβ/Smad signaling: To test the postulate that Smad3 gene deficiency impacts TGFβ/Smad signaling, the mRNA expression levels of TGFβ, Smad2, Smad4, and Smad7 were quantified in Smad3$^{-/-}$ mouse corneal tissue and compared with Smad3$^{+/+}$ mouse corneal tissue during active wound healing (Figure 8). The results of the mRNA expression study revealed a significant alteration in TGFβ (Figure 8A; $p<0.01$), Smad2 (Figure 8B; $p<0.01$), Smad4 (Figure 8C; $p<0.05$), and Smad7 (Figure 8D; $p<0.01$) and evidenced the role of Smad3 in TGFβ/Smad signaling. The mRNA expression of TGFβ and Smad reveals that Smad3 gene deficiency directly regulates profibrotic cascades during active wound healing.

Effects of Smad3 deficiency on MMP/TIMP expression during corneal wound healing: MMPs and TIMPs critically regulate the active wound-healing event. To consider this, we examined the effect of Smad3 gene deficiency on MMP and TIMP expression during corneal wound healing in both Smad3$^{-/-}$ and Smad3$^{+/+}$ mouse corneal tissue (Figure 9). The Smad3$^{-/-}$ mouse corneal tissue showed lower MMP-1, MMP-2, and MMP-9 mRNA expressions ($p<0.001$) compared with the Smad3$^{+/+}$ mouse corneal tissue (Figure 9A). Additionally, the protein level western blot data analysis showed that MMPs and TIMPs were expressed at higher levels during the injury as compared with the naïve control in both groups, but in Smad3$^{-/-}$ mouse corneal tissue lysate, the expression was lower than in the Smad3$^{+/+}$ mouse corneal tissue lysate (Figure 9B). In addition, gelatin zymography showed both the pro and active forms of MMPs, and data were well corroborated with the mRNA and protein expression data (Figure 9C).

Smad3 expression increased in traumatic human corneal tissue: To validate and support our lead hypothesis—a direct role of Smad3 in cellular differentiation during corneal wound healing—donor human normal and traumatic corneal tissue sections were used for the assessment of Smad3 expression (Figure 10). The protein expression of Smad3 was increased notably in the traumatic donor human corneal tissue sections (Figure 10B) as compared with the corresponding control

nontraumatic donor human corneal tissue sections (Figure 10A). The increased Smad3 expression in the traumatic donor human corneal tissue aligns with our proposed hypothesis and shows the direct role of Smad3 during corneal wound healing.

DISCUSSION

Corneal injury involves orchestrated cellular growth factors and cytokine response to maintain physiologic homeostasis during active wound healing [1-7]. During active wound healing, many processes are involved, including the activation of fibroblasts and the reorganization and synthesis of the ECM [8-14]. The transparency of the corneal tissue is the key factor for normal vision. Disruption of the corneal transparency leads to vision impairment. Changes in corneal transparency are impacted by various ocular insults (e.g., mechanical, surgical, or chemical). These insults alter the transdifferentiation, production of various growth factors, cytokines, and excess accumulation of ECM proteins, leading to shifts in corneal curvature, myofibroblast formation, and collagen fibrillogenesis [8-14]. During traumatic injury, TGFβ can stimulate both canonical and noncanonical pathways involving TGFβRII, TGFβRI, BMP7, Smad2, Smad3, and Smad4 to affect a variety of cellular responses [23-31,52]. Smad intracellular proteins have the important role of transmitting TGFβ superfamily ligand signals to the nucleus [23-32]. In the TGFβ signaling pathway, the phosphorylation of R-Smads (Smad2 and Smad3) with co-Smad4

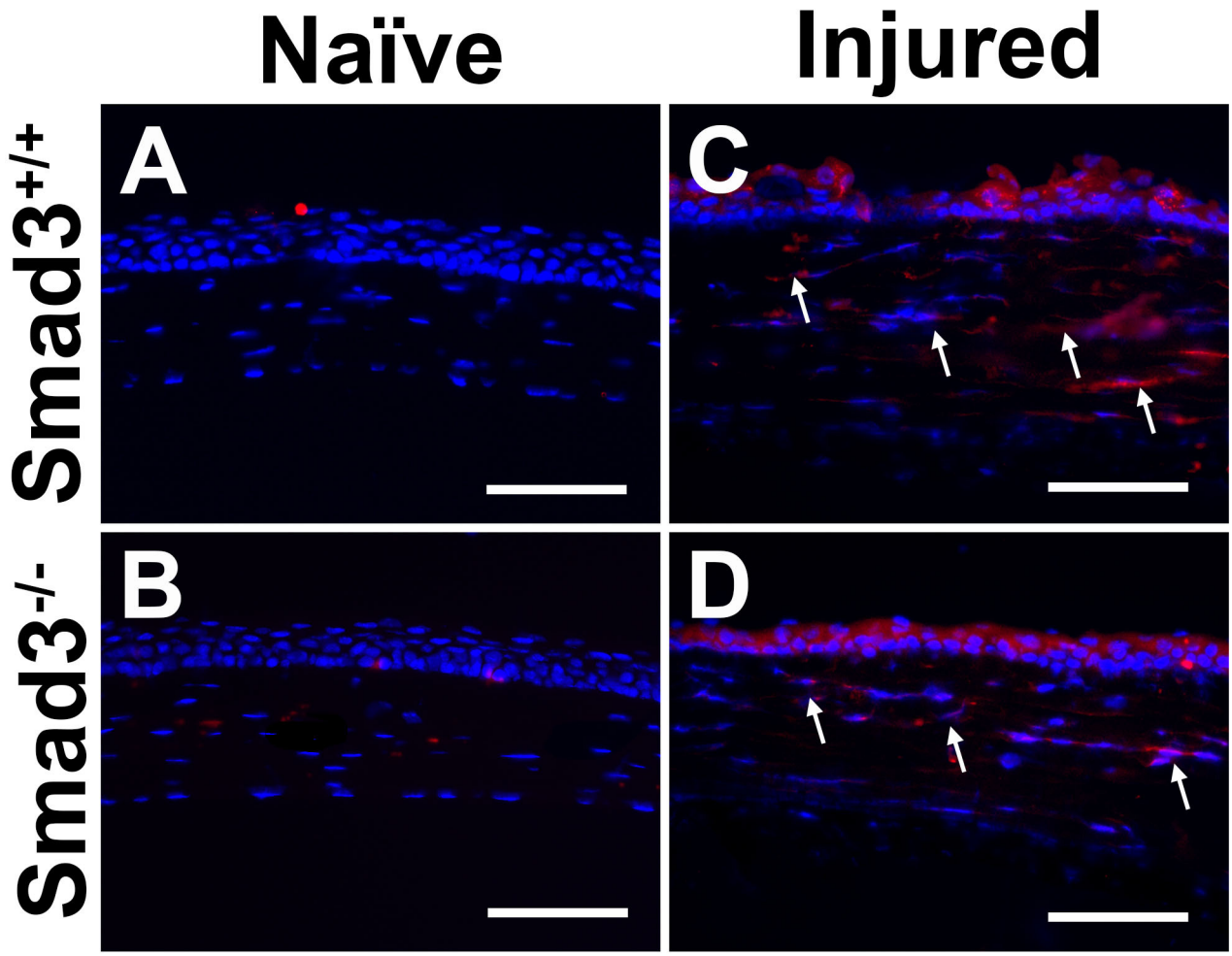

Figure 4. Smad3 gene deficiency tailored the inflammatory protein expression and impacted the corneal wound healing in mice after alkali injury. Expression of inflammatory protein CD11b expression in **A:** Smad3$^{+/+}$ naïve mouse corneal tissue; **B:** Smad3$^{-/-}$ naïve mouse corneal tissue; **C:** Smad3$^{+/+}$ alkali-injured mouse corneal tissue at day 21; and **D:** Smad3$^{-/-}$ alkali-injured mouse corneal tissue at day 21. The alkali injury increases the CD11b protein expression (arrow) in both strains of Smad3$^{+/+}$ and Smad3$^{-/-}$ mouse corneal tissue as compared with naïve control mouse corneal tissue, respectively. Scale bar = 200 µm.

and the translocation of this complex regulates the cellular transdifferentiation during the active wound healing that impacts the stromal regeneration and ECM remodeling [7,23-32,53]. Unlike other cytokines in the corneal tissue, TGFβ primarily regulates the ECM protein accumulation, collagens, and fibronectin synthesis and alters the MMP–TIMP balance during the different wound-healing phases [33-39]. Our research group and others showed that overexpression

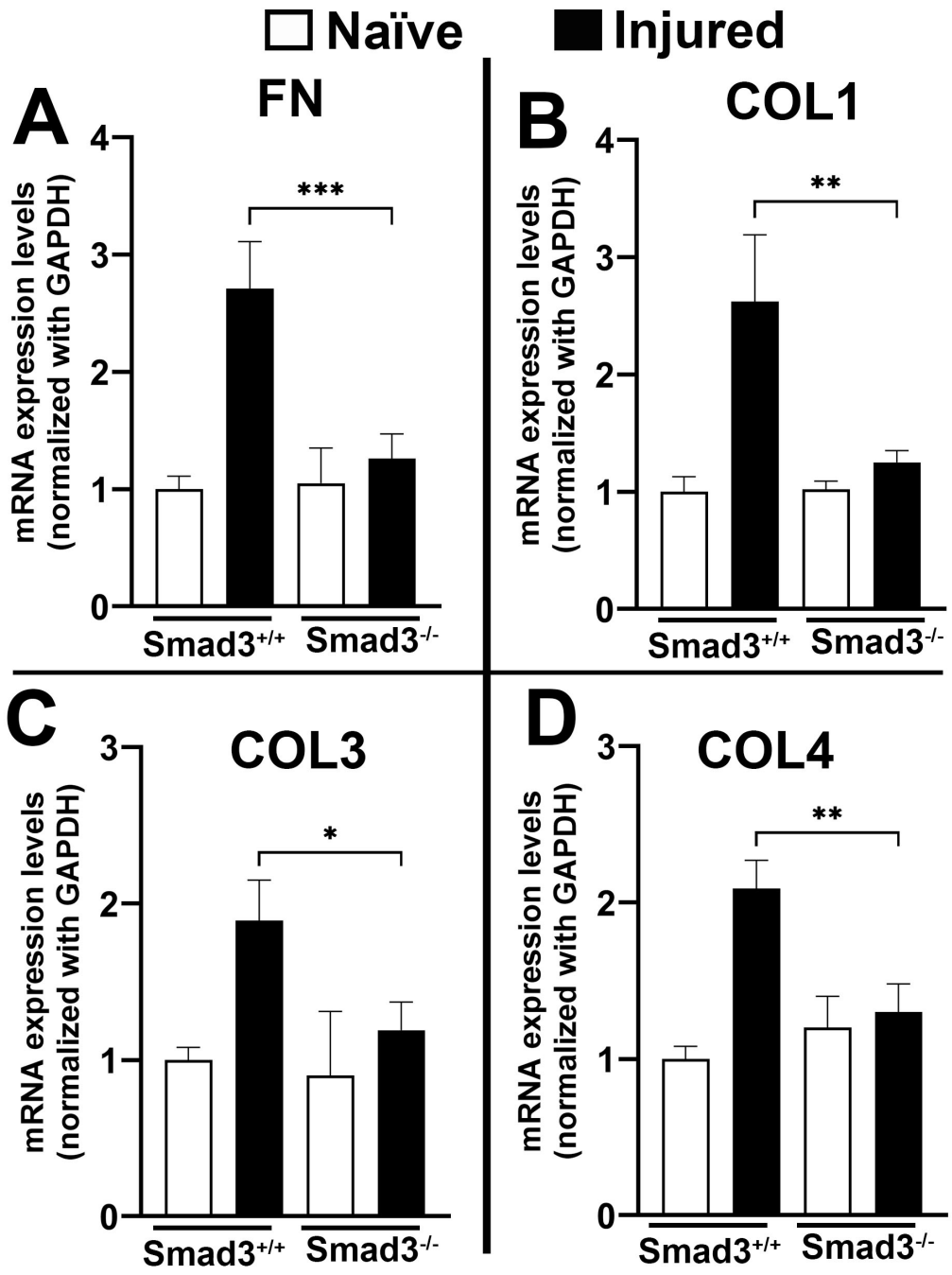

Figure 5. Smad3 gene deficiency suppresses the profibrotic gene expression and regulates stromal ECM protein modulation in mice after alkali injury. **A:** Fibronectin ($p<0.001$); **B:** collagen 1 ($p<0.01$); **C:** collagen 3 ($p<0.05$); and **D:** collagen IV ($p<0.01$) comparative mRNA expression of $Smad3^{-/-}$ mouse corneal tissue showed significantly reduced expression of profibrotic genes compared with $Smad3^{+/+}$ mouse corneal tissue after alkali injury. Results are expressed as mean ± SEM, and $p<0.05$ was considered significant. FN = Fibronectin; COL1 = Collagen 1; COL3 = Collagen 3; and COL4 = Collagen 4.

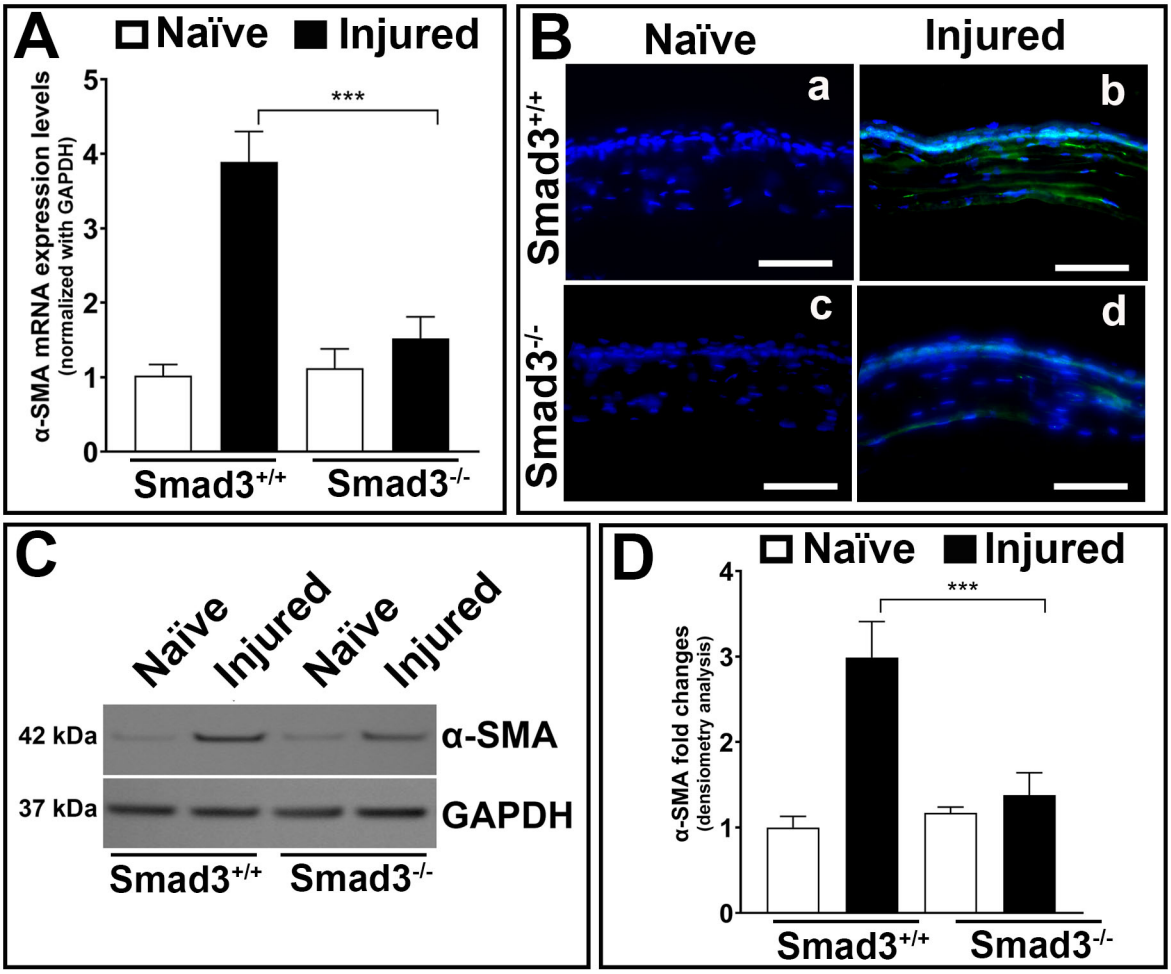

Figure 6. Smad3 gene deficiency regulates the stromal ECM protein modulation during fibrosis in mice after alkali injury. **A:** The comparative mRNA expression of α-SMA (fibrosis marker) was significantly downregulated in Smad3$^{-/-}$ mouse corneal tissue compared with Smad3$^{+/+}$ mouse corneal tissue after alkali injury. **B:** The immunofluorescence staining of α-SMA was prominently reduced in Smad3$^{-/-}$ mouse corneal tissue compared with Smad3$^{+/+}$ mouse corneal tissue after alkali injury, whereas no changes were recorded in both Smad3$^{+/+}$ and Smad3$^{-/-}$ mouse naïve corneal tissue sections. **C:** The western blot images showed that the α-SMA protein level was notably abridged in Smad3$^{-/-}$ mouse corneal tissue compared with Smad3$^{+/+}$ mouse corneal tissue after alkali injury, whereas no changes were recorded in both Smad3$^{+/+}$ and Smad3$^{-/-}$ mouse naïve corneal tissue sections. **D:** The western blot densitometry analysis graph shows a significant reduction in fibrosis level in Smad3$^{-/-}$ mouse corneas compared with Smad3$^{+/+}$ mouse corneas. The results are expressed as mean ± SEM, and $p<0.05$ was considered significant. Scale bar = 200 µm.

of BMP7 and Smad7 gene transfer via adenoviral vectors topically suppresses the alkali-induced fibrotic response in vivo and showed the translational perspective of Smads as a potential therapeutic target for corneal fibrosis [7,52-54]. In Smad-dependent transdifferentiation, the roles of Smad2 and Smad3 are apparent, as shown by various research groups: Smad2 null mutation leads to embryonic lethality, whereas mice lacking Smad3 survive [53-58]. In addition, corneal researchers have shown that the ablation of the Smad3 gene does not arrest epithelial repair in a mouse cornea [26,53,59]. To consider this, the direct role of Smad3 in corneal stromal wound healing and stromal remodeling required precise investigations. In these studies, we showed that corneal transparency was noticeably superior in the Smad3 gene ablated mouse corneas compared with the wild-type mouse corneas (Figure 2). The absence of the Smad3 gene did not impact the corneal transparency and corneal epithelium's regular turnover (Figure 3). No significant differences were reported in the IOP of both groups of animals (Table 2), reflecting that ablation of the Smad3 gene does not impact the flow of aqueous humor in ocular tissue. To better understand the functional role of Smad3, naïve and alkali-injured corneal tissue sections were evaluated for inflammatory protein (CD11b) after euthanasia on day 21 in wild-type and Smad3-deficient

mice. In general, wild-type (Smad3$^{+/+}$) alkali-injured corneas showed aggravated inflammatory responses compared with Smad3-deficient (Smad3$^{-/-}$) alkali-injured corneas (Figure 4). Our mRNA (Figure 5) and protein (Figure 6) data undoubtedly illustrated the role of Smad3 in alkali-driven stromal transdifferentiation and corneal fibrosis. Furthermore, Mason's trichrome staining confirmed and illustrated that Smad3 plays a critical role in ECM architecture, as shown by excessive collagen synthesis in the corneal tissue (Figure 7). The characteristic organization of stromal collagen fibrils provides mechanical strength and is required for the transparency of corneal tissue to maintain vision. The alterations in collagen levels in Smad3$^{+/+}$ compared with Smad3$^{-/-}$ revealed the direct role of Smad3 in stromal ECM protein modulation during active wound healing (Figure 7). TGFβ-activating mechanisms depend on receptor-activated Smads [7]. The relative mRNA expression profile of TGFβ and other Smads showed the rapport harmony of Smad3 on TGFβ/Smad signaling in wild-type and Smad-deficient mouse corneal tissue during naïve and alkali trauma conditions (Figure 8). Therefore, in a clinical setting, an approach that incorporates multiple modalities may have greater therapeutic efficiency. Smad3, in particular, has been shown to interact with Smad2 and oligomerize with co-Smads to form a heteromeric complex, thereby interacting with R-Smad-Smad4 oligomerization [7]. Disruption in a heteromeric complex of R-Smads has the potential to control the fibrosis cascade and serve as a potential target to regulate active wound healing. Collectively, our findings suggest that inhibition of Smad3 is an important aspect for regulating TGFβ1-mediated differentiation and ECM protein modulation, as shown by Smad3$^{-/-}$ deficient mice during alkali trauma.

In the past, our research group and others showed the critical role of MMPs in wound healing and ECM matrix remodeling [25,33-39]. This study supports our previous findings that both the pro- and active MMPs are involved during the active phase of wound healing. Increased MMP and TIMP expression levels were also found during the corneal stromal fibroblast to myofibroblast transdifferentiation (Figure 9). The crosstalk of Smad3 with the regulation of MMP and TIMP levels is another important aspect of the degradation and remodeling of the stromal ECM and modulation of stromal opacification [33-39]. These findings agree with other research showing that the ECM components expression, stromal reorganization, and collagen fibrillogenesis depend on Smad3 [20,25,29,33-39]. In the ECM protein

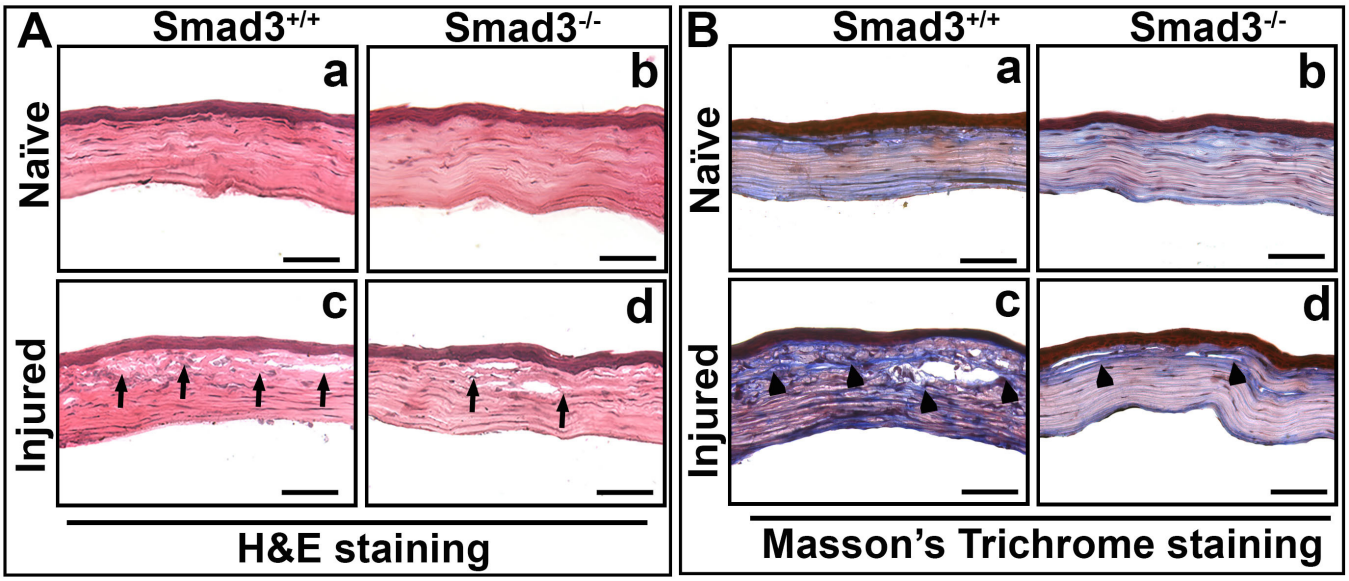

Figure 7. Smad3 directly associated with stromal ECM protein modulation impacted the corneal stromal wound healing in mice after alkali injury during active wound healing. **A**: H&E staining showing the morphological architecture of Smad3$^{+/+}$ naïve (a); Smad3$^{-/-}$ naïve (b); Smad3$^{+/+}$ post-alkali injury (c); and Smad3$^{-/-}$ post-alkali injury (d) corneal tissue sections at day 21. No structural changes were observed in Smad3$^{-/-}$ and Smad3$^{+/+}$ naïve corneal tissue sections. An increased cellular infiltration and distorted collagen lamellae (arrows) were observed in the corneal stroma of Smad3$^{+/+}$ and Smad3$^{-/-}$ compared with Smad3$^{-/-}$ mouse corneal tissue sections after alkali injury at day 21. **B**: Masson's trichrome staining showed the gross collagen level in Smad3$^{+/+}$ naïve (a); Smad3$^{-/-}$ naïve (b); Smad3$^{+/+}$ post-alkali injury (c); and Smad3$^{-/-}$ post-alkali injury (d) corneal tissue sections at day 21. No collagen levels were altered in Smad3$^{-/-}$ and Smad3$^{+/+}$ naïve corneal tissue sections. Increased collagen deposition was observed in the corneal stroma of Smad3$^{+/+}$ compared with Smad3$^{-/-}$ mouse corneal tissue sections after alkali injury at day 21, as indicated by increased blue color intensity (arrowhead). Scale bar = 200 µm.

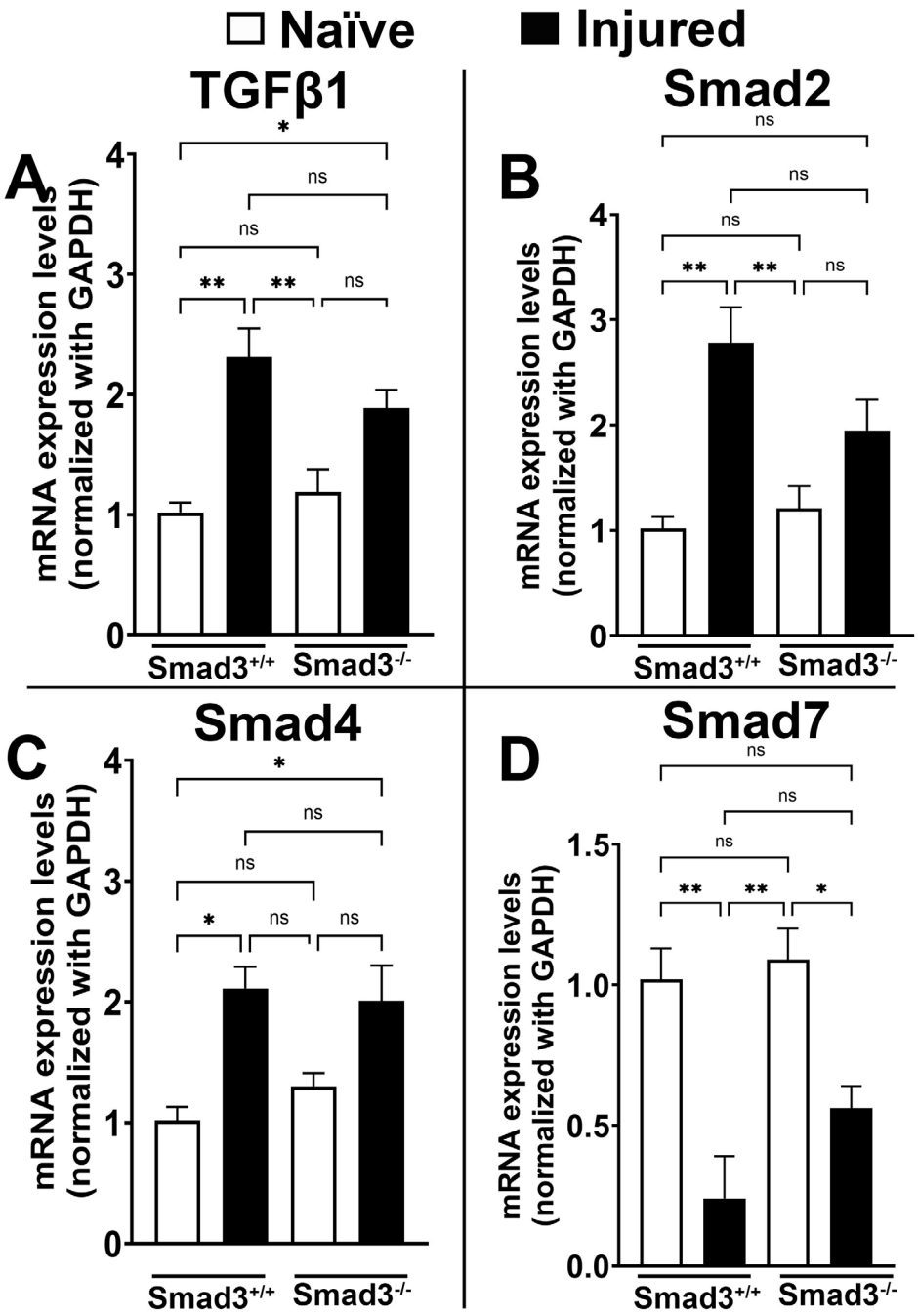

Figure 8. Effects of Smad3 gene deficiency in TGFβ/Smad signaling in mice after alkali injury. **A:** TGFβ1 ($p<0.001$); **B:** Smad2 ($p<0.01$); **C:** Smad4 ($p<0.05$); and **D:** Smad7 comparative mRNA expression significantly altered in post-alkali injury tissue at day 21 in both $Smad3^{+/+}$ and $Smad3^{-/-}$ strains as compared with corresponding naïve control mouse corneal tissue. Results are expressed as mean ± SEM, and $p<0.05$ was considered significant. (*$p<0.05$, ***$p<0.01$, and ns = not significant).

modulation, the MMPs and collagens play a decisive role during corneal wound healing, and our finding regarding Smad3 gene deficiency showed the direct relationship between Smad3, collagen, and MMP expression in the cornea (Figure 9). The expression of matrix metalloproteinase-2 is Smad2-dependent. Saika et al. and others showed that in the cornea, extirpation of the Smad3 gene had a similar anti-profibrogenic effect in the healing after an alkali burn in mice [25-27,53,54,59-64]. The results of this work agree with our previous work and other investigators' work showing that the

overexpression of Smad7 (inhibitory Smad) blocks the TGFβ/Smad-driven transdifferentiation of keratocytes to myofibroblast transformation and Smad-driven ECM remodeling and collagen fibrillogenesis [7,12,21,26-28,31,53-60]. The literature shows that the TGFβR-II phosphorylates the MH2 domains of Smad3, and translocation of the phosphorylated

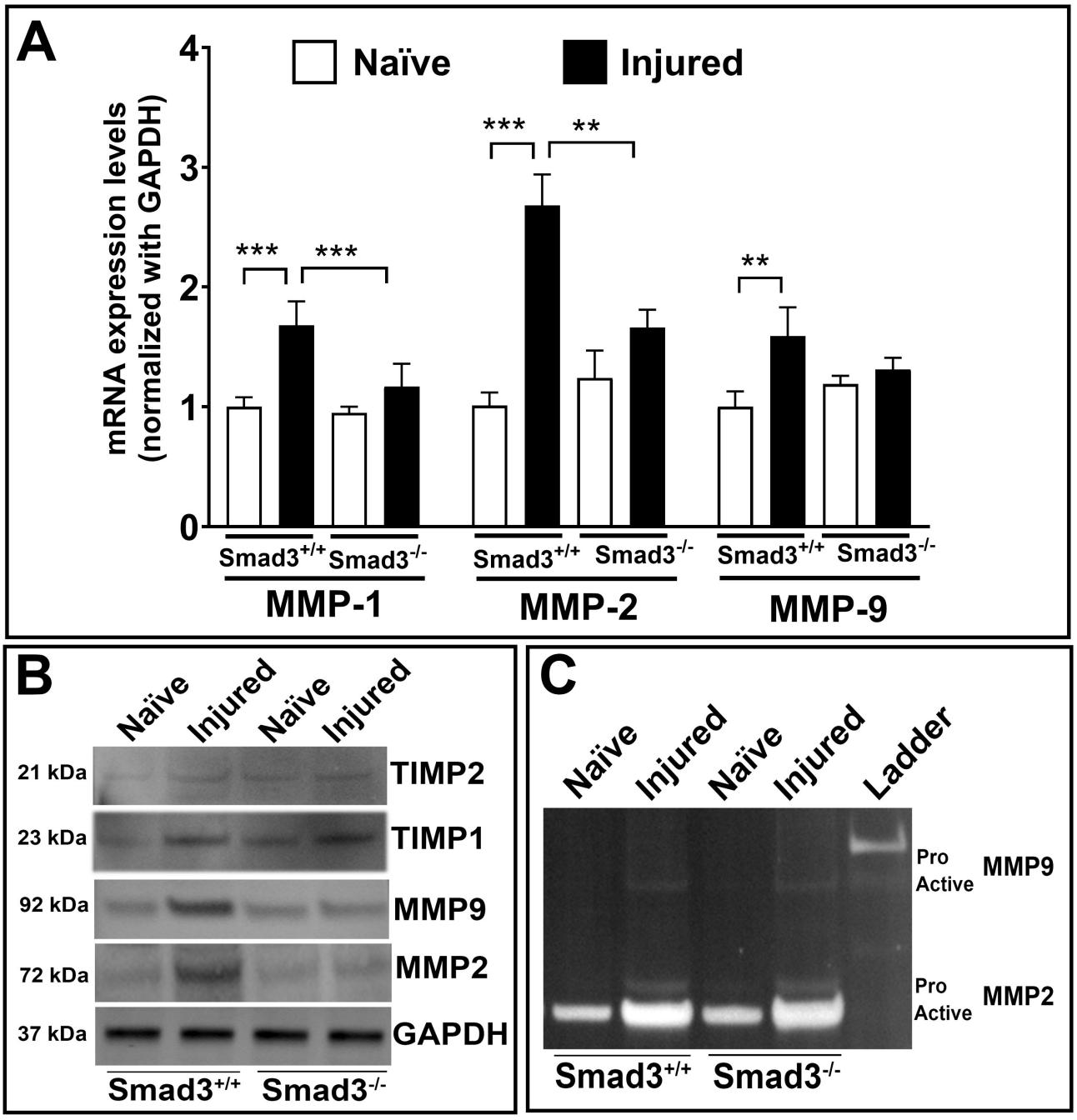

Figure 9. Smad3 gene deficiency impacted stromal ECM protein modulation via MMP and TIMP expression during active wound healing in mice after alkali injury. **A:** The comparative mRNA expressions of MMP1, MMP2, and MMP9 showed significantly reduced expression in Smad3$^{-/-}$ mouse corneal tissue after alkali injury compared with Smad3$^{+/+}$ mouse corneal tissue after alkali injury. **B:** The western blot showed similar trends of MMP and TIMP expression in the corneal tissue lysate of Smad3$^{-/-}$ mice compared with Smad3$^{+/+}$ mouse corneal tissue lysate. **C:** Gelatin zymography showed the pro and active MMP patterns in the corneal tissue lysate of Smad3$^{-/-}$ mice compared with Smad3$^{+/+}$ mouse corneal tissue lysate. The results are expressed as mean ± SEM, and $p<0.05$ was considered significant.

Smad complex regulates transdifferentiation during corneal fibrosis [60-66]. Our donor human corneal tissue data from the traumatic and nontraumatic samples further support and validate the proposed hypothesis and show the role of Smad3 in corneal wound healing (Figure 10). Taken together, a significant increase in profibrotic genes (α-SMA and FN), changes in collagen levels, MMPs (ECM regulatory enzymes), and changes in TGFβ1 expression depict the direct role of Smad3 in corneal wound healing and stromal remodeling, in agreement with the findings of other corneal researchers showing that phosphorylated Smad3 binds directly to the promoter region of the COL1A2 gene to activate transcription in embryonic mouse dermal fibroblasts [67-69].

In conclusion, this study reveals a direct role of Smad3 in the TGFβ1-mediated cascade that influences transdifferentiation of stromal keratocyte/fibroblasts to opaque myofibroblasts during corneal wound healing. Additionally, it highlights that Smad3 is a promising target for controlling abnormal corneal wound healing and fibrosis in vivo. However, additional research is required for a better mechanistic understanding of Smad3's role in the treatment of fibrosis in ocular and non-ocular tissues.

ACKNOWLEDGMENTS

This work was supported by the 1I01BX000357 Merit and IK6BX005646 SRCS awards (R.R.M.) from the United States Department of Veterans Affairs BLR&D, Washington DC, USA; R01EY017294 and R01EY030774 grants (R.R.M.) from the National Eye Institute, NIH, Bethesda, Maryland, USA; and University of Missouri Ruth M. Kraeuchi Missouri Endowed Chair Ophthalmology Fund (RRM). Disclaimer: The contents do not represent the views of the USA Department of Veterans Affairs or the United States Government. Declaration of competing interest: None of the authors have any conflict of interest to disclose. Availability of data and materials: The data sets used and/or analyzed during the current study are available from the corresponding author upon reasonable request.

REFERENCES

1. Bukowiecki A, Hos D, Cursiefen C, Eming SA. Wound-Healing Studies in Cornea and Skin: Parallels, Differences and Opportunities. Int J Mol Sci 2017; 18:1257-[PMID: 28604651].

2. Ghafar NA, Jalil NAA, Kamarudin TA. Wound healing of the corneal epithelium: a review. Asian Biomed (Res Rev News) 2021; 15:199-212. Res Rev News[PMID: 37551323].

3. Mohan RR, Gupta S, Kumar R, Sinha NR, Landreneau J, Sinha PR, Tandon A, Chaurasia SS, Hesemann NP. Tissue-targeted and localized AAV5-DCN and AAV5-PEDF combination gene therapy abrogates corneal fibrosis and concurrent neovascularization in rabbit eyes *in vivo*. Ocul Surf 2024; 32:13-25. [PMID: 38191093].

4. Wilson SL, El Haj AJ, Yang Y. Control of scar tissue formation in the cornea: strategies in clinical and corneal tissue engineering. J Funct Biomater 2012; 3:642-87. [PMID: 24955637].

5. Stern JH, Tian Y, Funderburgh J, Pellegrini G, Zhang K, Goldberg JL, Ali RR, Young M, Xie Y, Temple S. Regenerating eye tissues to preserve and restore vision. Cell Stem Cell 2018; 22:834-49. [PMID: 29859174].

6. Gupta S, Fink MK, Kempuraj D, Sinha NR, Martin LM, Keele LM, Sinha PR, Giuliano EA, Hesemann NP, Raikwar SP, Chaurasia SS, Mohan RR. Corneal fibrosis abrogation by a localized AAV-mediated inhibitor of differentiation 3 (Id3) gene therapy in rabbit eyes *in vivo*. Mol Ther 2022; 30:3257-69. [PMID: 35780298].

7. Gupta S, Rodier JT, Sharma A, Giuliano EA, Sinha PR, Hesemann NP, Ghosh A, Mohan RR. Targeted AAV5-Smad7 gene therapy inhibits corneal scarring *in vivo*. PLoS One 2017; 12:e0172928[PMID: 28339457].

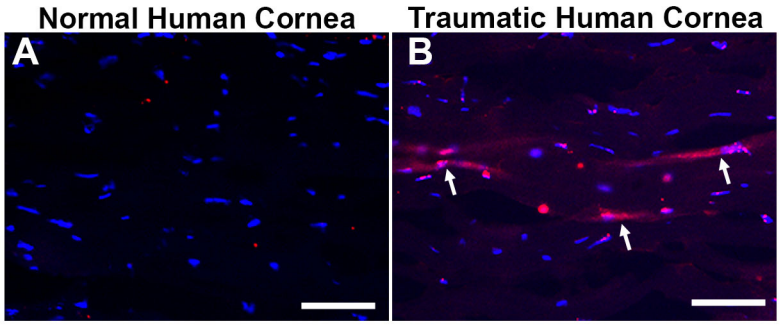

Figure 10. Enhanced Smad3 expression during the post-trauma period played a critical role during wound healing. **A:** Smad3 level in normal donor human cornea. **B:** Smad3 level in traumatic human cornea. The Smad3 levels were remarkably increased (arrow) in the post-trauma donor human cornea as compared with the normal donor human cornea. Scale bar = 200 µm.

8. Gupta S, Fink MK, Martin LM, Sinha PR, Rodier JT, Sinha NR, Hesemann NP, Chaurasia SS, Mohan RR. A rabbit model for evaluating ocular damage from acrolein toxicity *in vivo.* Ann N Y Acad Sci 2020; 480:233-45. .
9. Wilson SE. Corneal myofibroblasts and fibrosis. Exp Eye Res 2020; 201:108272[PMID: 33010289].
10. Gupta S, Martin LM, Sinha NR, Smith KE, Sinha PR, Dailey EM, Hesemann NP, Mohan RR. Role of *inhibitor of differentiation 3 gene* in cellular differentiation of human corneal stromal fibroblasts. Mol Vis 2020; 26:742-56. [PMID: 33273801].
11. van der Putten C, van den Broek D, Kurniawan NA. Myofibroblast transdifferentiation of keratocytes results in slower migration and lower sensitivity to mesoscale curvatures. Front Cell Dev Biol 2022; 10:930373[PMID: 35938166].
12. Gupta S, Buyank F, Sinha NR, Grant DG, Sinha PR, Iozzo RV, Chaurasia SS, Mohan RR. Decorin regulates collagen fibrillogenesis during corneal wound healing in mouse *in vivo.* Exp Eye Res 2022; 216:108933[PMID: 35031282].
13. Diller RB, Tabor AJ. The role of the extracellular matrix (ECM) in wound Healing: A review. Biomimetics (Basel) 2022; 7:87-[PMID: 35892357].
14. Moretti L, Stalfort J, Barker TH, Abebayehu D. The interplay of fibroblasts, the extracellular matrix, and inflammation in scar formation. J Biol Chem 2022; 298:101530[PMID: 34953859].
15. Congdon N, O'Colmain B, Klaver CC, Klein R, Muñoz B, Friedman DS, Kempen J, Taylor HR, Mitchell P. Eye Diseases Prevalence Research Group. Causes and prevalence of visual impairment among adults in the United States. Arch Ophthalmol 2004; 122:477-85. [PMID: 15078664].
16. . Global Burden of Disease Study 2013 Collaborators. Global, regional, and national incidence, prevalence, and years lived with disability for 301 acute and chronic diseases and injuries in 188 countries, 1990-2013: a systematic analysis for the Global Burden of Disease Study 2013. Lancet 2015; 386:743-800. [PMID: 26063472].
17. Robaei D, Watson S. Corneal blindness: a global problem. Clin Exp Ophthalmol 2014; 42:213-4. .[PMID: 24734984].
18. Gupta S, Kamil S, Sinha PR, Rodier JT, Chaurasia SS, Mohan RR. Glutathione is a potential therapeutic target for acrolein toxicity in the cornea. Toxicol Lett 2021; 340:33-42. [PMID: 33421550].
19. Solebo AL, Teoh L, Rahi J. Epidemiology of blindness in children. Arch Dis Child 2017; 102:853-7. [PMID: 28465303].
20. Tidke SC, Tidake P. A Review of Corneal Blindness: Causes and Management. Cureus 2022; 14:e30097[PMID: 36381769].
21. Sinha NR, Balne PK, Bunyak F, Hofmann AC, Lim RR, Mohan RR, Chaurasia SS. Collagen matrix perturbations in corneal stroma of Ossabaw mini pigs with type 2 diabetes. Mol Vis 2021; 27:666-78. [PMID: 35002212].
22. Gouveia RM, Lepert G, Gupta S, Mohan RR, Paterson C, Connon CJ. Assessment of corneal substrate biomechanics and its effect on epithelial stem cell maintenance and differentiation. Nat Commun 2019; 10:1496-[PMID: 30944320].
23. Arany PR, Flanders KC, Kobayashi T, Kuo CK, Stuelten C, Desai KV, Tuan R, Rennard SI, Roberts AB. Smad3 deficiency alters key structural elements of the extracellular matrix and mechanotransduction of wound closure. Proc Natl Acad Sci U S A 2006; 103:9250-5. [PMID: 16754864].
24. Saika S. TGF-beta signal transduction in corneal wound healing as a therapeutic target. Cornea 2004; 23:S25-30. [PMID: 15448476].
25. Gronkiewicz KM, Giuliano EA, Sharma A, Mohan RR. Molecular mechanisms of suberoylanilide hydroxamic acid in the inhibition of TGF-β1-mediated canine corneal fibrosis. Vet Ophthalmol 2016; 19:480-7. [PMID: 26559782].
26. Saika S, Yamanaka O, Okada Y, Sumioka T. Modulation of Smad signaling by non-TGFβ components in myofibroblast generation during wound healing in corneal stroma. Exp Eye Res 2016; 142:40-8. [PMID: 26675402].
27. Miyazono K. TGF-beta signaling by Smad proteins. Cytokine Growth Factor Rev 2000; 11:15-22. [PMID: 10708949].
28. Finnson KW, Almadani Y, Philip A. Non-canonical (non-SMAD2/3) TGF-β signaling in fibrosis: Mechanisms and targets. Semin Cell Dev Biol 2020; 101:115-22. [PMID: 31883994].
29. Dennler S, Itoh S, Vivien D, ten Dijke P, Huet S, Gauthier JM. Direct binding of Smad3 and Smad4 to critical TGF beta-inducible elements in the promoter of human plasminogen activator inhibitor-type 1 gene. EMBO J 1998; 17:3091-100. [PMID: 9606191].
30. Nelson EF, Huang CW, Ewel JM, Chang AA, Yuan C. Halofuginone down-regulates Smad3 expression and inhibits the TGFbeta-induced expression of fibrotic markers in human corneal fibroblasts. Mol Vis 2012; 18:479-87. [PMID: 22393274].
31. Sinha NR, Tripathi R, Balne PK, Suleiman L, Simkins K, Chaurasia SS, Mohan RR. Mustard gas exposure actuates SMAD2/3 signaling to promote myofibroblast generation in the cornea. Cells 2023; 12:1533-[PMID: 37296653].
32. Xu P, Lin X, Feng XH. Posttranslational Regulation of Smads. Cold Spring Harb Perspect Biol 2016; 8:a022087[PMID: 27908935].
33. Wolf M, Clay SM, Oldenburg CE, Rose-Nussbaumer J, Hwang DG, Chan MF. Overexpression of MMPs in corneas requiring penetrating and deep anterior lamellar keratoplasty. Invest Ophthalmol Vis Sci 2019; 60:1734-47. [PMID: 31022731].
34. Ra HJ, Parks WC. Control of matrix metalloproteinase catalytic activity. Matrix Biol 2007; 26:587-96. [PMID: 17669641].
35. Mulholland B, Tuft SJ, Khaw PT. Matrix metalloproteinase distribution during early corneal wound healing. Eye (Lond) 2005; 19:584-8. [PMID: 15332107].
36. Leivonen SK, Lazaridis K, Decock J, Chantry A, Edwards DR, Kähäri VM. TGF-β-elicited induction of tissue inhibitor of metalloproteinases (TIMP)-3 expression in fibroblasts

involves complex interplay between Smad3, p38α, and ERK1/2. PLoS One 2013; 8:e57474[PMID: 23468994].

37. Zhou X, Hu H, Huynh ML, Kotaru C, Balzar S, Trudeau JB, Wenzel SE. Mechanisms of tissue inhibitor of metalloproteinase 1 augmentation by IL-13 on TGF-beta 1-stimulated primary human fibroblasts. J Allergy Clin Immunol 2007; 119:1388-97. [PMID: 17418380].

38. Jia HZ, Pang X, Peng XJ. Changes of matrix metalloproteinases in the stroma after corneal cross-linking in rabbits. Int J Ophthalmol 2021; 14:26-31. [PMID: 33469480].

39. García-López C, Rodríguez-Calvo-de-Mora M, Borroni D, Sánchez-González JM, Romano V, Rocha-de-Lossada C. The role of matrix metalloproteinases in infectious corneal ulcers. Surv Ophthalmol 2023; 68:929-39. [PMID: 37352980].

40. Tripathi R, Giuliano EA, Gafen HB, Gupta S, Martin LM, Sinha PR, Rodier JT, Fink MK, Hesemann NP, Chaurasia SS, Mohan RR. Is sex a biological variable in corneal wound healing? Exp Eye Res 2019; 187:107705[PMID: 31226339].

41. Ericsson AC, Myles M, Davis W, Ma L, Lewis M, Maggio-Price L, Franklin C. Noninvasive detection of inflammation-associated colon cancer in a mouse model. Neoplasia 2010; 12:1054-65. [PMID: 21170269].

42. Balne PK, Gupta S, Landon KM, Sinha NR, Hofmann AC, Hauser N, Sinha PR, Huang H, Kempuraj D, Mohan RR. Characterization of C-X-C chemokine receptor type 5 in the cornea and role in the inflammatory response after corneal injury. Exp Eye Res 2023; 226:[PMID: 36400287].

43. Anumanthan G, Gupta S, Fink MK, Hesemann NP, Bowles DK, McDaniel LM, Muhammad M, Mohan RR. KCa3.1 ion channel: A novel therapeutic target for corneal fibrosis. PLoS One 2018; 13:e0192145[PMID: 29554088].

44. Balne PK, Gupta S, Zhang J, Bristow D, Faubion M, Heil SD, Sinha PR, Green SL, Iozzo RV, Mohan RR. The functional role of decorin in corneal neovascularization in vivo. Exp Eye Res 2021; 207:108610[PMID: 33940009].

45. Anumanthan G, Sharma A, Waggoner M, Hamm CW, Gupta S, Hesemann NP, Mohan RR. Efficacy and safety comparison between suberoylanilide hydroxamic acid and mitomycin C in reducing the risk of corneal haze after PRK treatment *in vivo.* J Refract Surg 2017; 33:834-9. [PMID: 29227512].

46. Gupta S, Fink MK, Ghosh A, Tripathi R, Sinha PR, Sharma A, Hesemann NP, Chaurasia SS, Giuliano EA, Mohan RR. Novel combination BMP7 and HGF gene therapy instigates selective myofibroblast apoptosis and reduces corneal haze *in vivo.* Invest Ophthalmol Vis Sci 2018; 59:1045-57. [PMID: 29490341].

47. Zhang E, Gupta S, Olson E, Sinha PR, Hesemann NP, Fraunfelder FW, Mohan RR. Effects of regular/dilute proparacaine anesthetic eye drops in combination with ophthalmic antibiotics on corneal wound healing. J Ocul Pharmacol Ther 2022; 38:232-9. [PMID: 35275738].

48. Mohan RR, Balne PK, Muayad MS, Tripathi R, Sinha NR, Gupta S, An JA, Sinha PR, Hesemann NP. Six-month *in vivo* safety profiling of topical ocular AAV5-decorin gene transfer. Transl Vis Sci Technol 2021; 10:5-[PMID: 34383877].

49. Gupta S, Sinha NR, Martin LM, Keele LM, Sinha PR, Rodier JT, Landreneau JR, Hesemann NP, Mohan RR. Long-term safety and tolerability of BMP7 and HGF gene overexpression in rabbit cornea. Transl Vis Sci Technol 2021; 10:6-[PMID: 34383876].

50. Sharma A, Anumanthan G, Reyes M, Chen H, Brubaker JW, Siddiqui S, Gupta S, Rieger FG, Mohan RR. Epigenetic modification prevents excessive wound healing and scar formation after glaucoma filtration surgery. Invest Ophthalmol Vis Sci 2016; 57:3381-9. [PMID: 27367506].

51. Gupta S, Martin LM, Zhang E, Sinha PR, Landreneau J, Sinha NR, Hesemann NP, Mohan RR. Toxicological effects of ocular acrolein exposure to eyelids in rabbits *in vivo.* Exp Eye Res 2023; 234:109575[PMID: 37451567].

52. Tandon A, Sharma A, Rodier JT, Klibanov AM, Rieger FG, Mohan RR. BMP7 gene transfer via gold nanoparticles into stroma inhibits corneal fibrosis in vivo. PLoS One 2013; 8:e66434[PMID: 23799103].

53. Saika S, Ikeda K, Yamanaka O, Miyamoto T, Ohnishi Y, Sato M, Muragaki Y, Ooshima A, Nakajima Y, Kao WW, Flanders KC, Roberts AB. Expression of Smad7 in mouse eyes accelerates healing of corneal tissue after exposure to alkali. Am J Pathol 2005; 166:1405-18. [PMID: 15855641].

54. Saika S, Ikeda K, Yamanaka O, Flanders KC, Nakajima Y, Miyamoto T, Ohnishi Y, Kao WW, Muragaki Y, Ooshima A. Therapeutic effects of adenoviral gene transfer of bone morphogenic protein-7 on a corneal alkali injury model in mice. Lab Invest 2005; 85:474-86. [PMID: 15696184].

55. Flanders KC, Sullivan CD, Fujii M, Sowers A, Anzano MA, Arabshahi A, Major C, Deng C, Russo A, Mitchell JB, Roberts AB. Mice lacking Smad3 are protected against cutaneous injury induced by ionizing radiation. Am J Pathol 2002; 160:1057-68. [PMID: 11891202].

56. Datto MB, Frederick JP, Pan L, Borton AJ, Zhuang Y, Wang XF. Targeted disruption of Smad3 reveals an essential role in transforming growth factor beta-mediated signal transduction. Mol Cell Biol 1999; 19:2495-504. [PMID: 10082515].

57. Liu L, Liu X, Ren X, Tian Y, Chen Z, Xu X, Du Y, Jiang C, Fang Y, Liu Z, Fan B, Zhang Q, Jin G, Yang X, Zhang X. Smad2 and Smad3 have differential sensitivity in relaying TGFβ signaling and inversely regulate early lineage specification. Sci Rep 2016; 6:21602-[PMID: 26905010].

58. Mullen AC, Wrana JL. TGF-β Family Signaling in Embryonic and Somatic Stem-Cell Renewal and Differentiation. Cold Spring Harb Perspect Biol 2017; 9:a022186[PMID: 28108485].

59. Saika S, Kono-Saika S, Ohnishi Y, Sato M, Muragaki Y, Ooshima A, Flanders KC, Yoo J, Anzano M, Liu CY, Kao WW, Roberts AB. Smad3 signaling is required for epithelial-mesenchymal transition of lens epithelium after injury. Am J Pathol 2004; 164:651-63. [PMID: 14742269].

60. Sarenac T, Trapecar M, Gradisnik L, Rupnik MS, Pahor D. Single-cell analysis reveals IGF-1 potentiation of inhibition of the TGF-β/Smad pathway of fibrosis in human keratocytes in vitro. Sci Rep 2016; 6:34373-[PMID: 27687492].

61. Rosa I, Fioretto BS, Romano E, Buzzi M, Mencucci R, Marini M, Manetti M. The Soluble Guanylate Cyclase Stimulator BAY 41-2272 Attenuates Transforming Growth Factor β1-Induced Myofibroblast Differentiation of Human Corneal Keratocytes. Int J Mol Sci 2022; 23:15325-[PMID: 36499651].

62. Sugioka K, Nishida T, Kodama-Takahashi A, Murakami J, Mano F, Okada K, Fukuda M, Kusaka S. Urokinase-type plasminogen activator negatively regulates α-smooth muscle actin expression via Endo180 and the uPA receptor in corneal fibroblasts. Am J Physiol Cell Physiol 2022; 323:C104-15. [PMID: 35649252].

63. Stramer BM, Austin JS, Roberts AB, Fini ME. Selective reduction of fibrotic markers in repairing corneas of mice deficient in Smad3. J Cell Physiol 2005; 203:226-32. [PMID: 15521071].

64. Shen X, Hu PP, Liberati NT, Datto MB, Frederick JP, Wang XF. TGF-beta-induced phosphorylation of Smad3 regulates its interaction with coactivator p300/CREB-binding protein. Mol Biol Cell 1998; 9:3309-19. [PMID: 9843571].

65. Tandon A, Tovey JC, Sharma A, Gupta R, Mohan RR. Role of transforming growth factor Beta in corneal function, biology and pathology. Curr Mol Med 2010; 10:565-78. [PMID: 20642439].

66. Nakao A, Imamura T, Souchelnytskyi S, Kawabata M, Ishisaki A, Oeda E, Tamaki K, Hanai J, Heldin CH, Miyazono K, ten Dijke P. TGF-beta receptor-mediated signalling through Smad2, Smad3 and Smad4. EMBO J 1997; 16:5353-62. [PMID: 9311995].

67. McGaha TL, Kodera T, Spiera H, Stan AC, Pines M, Bona CA. Halofuginone inhibition of COL1A2 promoter activity via a c-Jun-dependent mechanism. Arthritis Rheum 2002; 46:2748-61. [PMID: 12384935].

68. Goffin L, Seguin-Estévez Q, Alvarez M, Reith W, Chizzolini C. Transcriptional regulation of matrix metalloproteinase-1 and collagen 1A2 explains the anti-fibrotic effect exerted by proteasome inhibition in human dermal fibroblasts. Arthritis Res Ther 2010; 12:R73-[PMID: 20429888].

69. Ponticos M, Abraham D, Alexakis C, Lu QL, Black C, Partridge T, Bou-Gharios G. Col1a2 enhancer regulates collagen activity during development and in adult tissue repair. Matrix Biol 2004; 22:619-28. [PMID: 15062855].